Hindawi Publishing Corporation
Physics Research International
Volume 2011, Article ID 350540, 7 pages
doi:10.1155/2011/350540

Research Article

Computations of Ultrasonic Parameters in $Zr_{100-X}Sn_X$ Alloys

Pramod Kumar Yadawa

Department of Applied Physics, AMITY School of Engineering and Technology, Bijwasan, New Delhi 110 061, India

Correspondence should be addressed to Pramod Kumar Yadawa, pkyadawa@aset.amity.edu

Received 10 September 2010; Revised 24 March 2011; Accepted 2 May 2011

Academic Editor: Ashok Chatterjee

The ultrasonic properties like ultrasonic attenuation, sound velocity in the hexagonal $Zr_{100-X}Sn_X$ alloys have been studied along unique axis at room temperature. The second- and third-order elastic constants (SOEC & TOEC) have been calculated for these alloys using Lennard-Jones potential. The velocities V_L and V_{S1} have minima and maxima, respectively, at 45° with unique axis of the crystal, while V_{S2} increases with the angle from unique axis. The inconsistent behaviour of angle-dependent velocities is associated to the action of second-order elastic constants. Debye average sound velocities of these alloys are increasing with the angle and has maximum at 55° with unique axis at room temperature. Hence, when a sound wave travels at 55° with unique axis of these alloys, then the average sound velocity is found to be maximum. The mechanical and ultrasonic properties of these alloys will be better than pure Zr and Sn due to their high SOEC and ultrasonic velocity and low ultrasonic attenuation. The comparison of calculated ultrasonic parameters with available theoretical/experimental physical parameters gives information about classification of these alloys.

1. Introduction

Group IV transition metal zirconium (Zr) and its alloys are very important materials both from scientific and technological points of view. Scientifically, the electronic transfer between the broad sp band and the narrow d band is the driving force behind many structural and electronic transitions in these materials [1–3]. Technologically, these alloys have applications in the aerospace industry due to their light weight, static strength, and stiffness; they do not degrade rapidly as the temperature increases, and they also show oxidation resistance [4]. The mechanical properties of these alloys can be greatly improved by controlling the crystallographic phases present.

Static high-pressure experimental works indicate that, at room temperature and ambient pressure, Zr is a hexagonal close-packed (hcp) structure (α phase). At high temperature and zero pressure, it transforms martensitically into the body-centered cubic (bcc) structure (β phase) before reaching the melting temperature [5] while at room temperature and under pressure, the hcp phase transforms into another hexagonal structure.

The first form of tin is called grey tin (α-Sn) and is stable at temperature below 286.2 K. This form crystallizes in the diamond structure [6], in common with the lighter elements in column IV A of the periodic table. At temperature above 286.2 K, grey tin slowly turns into tin's second form, white tin. This second form (β-Sn) is a tetragonal distortion of diamond with two atoms per unit cell [7]. Tin is used to form many useful alloys.

Up to now, only a few theoretical methods have been applied successfully to calculate the elastic constants of α-Zr, such as the full potential linear muffin-tin orbital (FP-LMTO) method [8], the tight-binding (TB) approach [9], the embedded-atom (EAM) method [10], and the modified embedded-atom (MEAM) method [11, 12]. However, elastic constants of ZrSn alloys have not yet been reported.

Ultrasonic properties offer the possibility to detect and characterize microstructural properties, as well as flaws in materials, controlling materials behaviour based on physical mechanism to predict future performance of the materials. Various investigators have shown considerable interest on ultrasonic properties of metals and alloys. Wave propagation velocity is key parameter in ultrasonic characterization and

can provide information about crystallographic texture. The ultrasonic velocity is directly related to the elastic constants by the relationship $V = \sqrt{C/\rho}$, where C is the relevant elastic constants, and ρ is the density of that particular material. Also ultrasonic attenuation is very important physical parameter to characterize the material, which is well related to several physical quantities like thermal conductivity, specific heat, thermal energy density and higher-order elastic constants [13, 14]. The elastic constants provide valuable information about the bonding characteristic between adjacent atomic planes and the anisotropic character of the bonding and structural stability [15, 16].

Therefore, in this work I predict the ultrasonic properties of hexagonal-structured $Zr_{100-X}Sn_X$ alloys ($Zr_{82}Sn_{18}$: alloy 1; $Zr_{80}Sn_{20}$: alloy 2; $Zr_{78}Sn_{22}$: alloy 3; $Zr_{76}Sn_{24}$: alloy 4) at room temperature. The ultrasonic attenuation coefficient, acoustic coupling constants, higher-order elastic constants, thermal relaxation time, and ultrasonic wave velocities for these alloys for each direction of propagation of wave are calculated at 300 K. The calculated ultrasonic parameters are discussed with related thermophysical properties for the characterization of the chosen alloys. The obtained results are analyzed in comparison to other hexagonal-structured materials and alloys.

2. Theory

In the present investigation, the theory is divided into three parts.

2.1. Second- and Third-Order Elastic Constants. The elastic energy density (U) is function of the strain components.

$$U = F\left(e_{xx}; e_{yy}; e_{zz}; e_{yz}; e_{zx}; e_{xy}\right) = F(e_1; e_2; e_3; e_4; e_5; e_6), \quad (1)$$

where e_{ij} (i or $j = x, y, z$) is component of strain tensor.

The second- (C_{IJ}) and third- (C_{IJK}) order elastic constants of material are defined by following expressions.

$$C_{IJ} = \frac{\partial^2 U}{\partial e_I \partial e_J}, \quad I \text{ or } J = 1, \ldots, 6,$$
$$C_{IJK} = \frac{\partial^3 U}{\partial e_I \partial e_J \partial e_K}, \quad I \text{ or } J \text{ or } K = 1, \ldots, 6. \quad (2)$$

The elastic energy density is well related to interaction potential $\Phi(r)$ between atoms. Let the interaction potential be the Lennard-Jones Potential or many-body interaction potential, which is formulated as:

$$\Phi(r) = -\frac{a_0}{r^m} + \frac{b_0}{r^n}, \quad (3)$$

where a_0, b_0 are constants, and m, n are integers. The definition of higher order elastic constants (2) with this potential (3) under equilibrium and symmetric condition six second- and ten third-order elastic constants (SOEC and TOEC) for the hexagonal closed packed structured materials [13, 17]

$$\begin{aligned}
C_{11} &= 24.1p^4C', \qquad C_{12} = 5.918p^4C',\\
C_{13} &= 1.925p^6C', \qquad C_{33} = 3.464p^8C',\\
C_{44} &= 2.309p^4C', \qquad C_{66} = 9.851p^4C',\\
C_{111} &= 126.9p^2B + 8.853p^4C',\\
C_{112} &= 19.168p^2B - 1.61p^4C',\\
C_{113} &= 1.924p^4B + 1.155p^6C',\\
C_{123} &= 1.617p^4B - 1.155p^6C',\\
C_{133} &= 3.695p^6B, \qquad C_{155} = 1.539p^4B,\\
C_{144} &= 2.309p^4B, \qquad C_{344} = 3.464p^6B,\\
C_{222} &= 101.039p^2B + 9.007p^4C',\\
C_{333} &= 5.196p^8B,
\end{aligned} \quad (4)$$

where $p = c/a$; axial ratio; $C' = \chi a/p^5$; $B = \psi a^3/p^3$. The rest second-order elastic constants have zero value because under 180° rotation, they have equal and opposite value for the same stress. The harmonic and anharmonic parameters (χ and ψ) can be calculated using one experimental SOEC [13, 17]. In the present study, I have expanded the theory for theoretical evaluation of parameters χ and ψ. The potential energy can be expanded in the powers of changes in the squares of distances. The expansion up to cubic term can be written as:

$$\Phi = \Phi_0 + \chi \sum_{i=1}^{2} \left[\Delta r_i^2\right]^2 + \psi \sum_{i=1}^{2} \left[\Delta r_i^2\right]^3. \quad (5)$$

According to (5), χ and ψ can be written as:

$$\chi = \frac{1}{2!}\left[\frac{d^2\Phi(r)}{d(r^2)^2}\right],$$
$$\psi = \frac{1}{3!}\left[\frac{d^3\Phi(r)}{d(r^2)^3}\right]. \quad (6)$$

In solving (6) for hexagonal closed packed structured materials:

$$\chi = \left(\frac{1}{8}\right)\left[\frac{\{nb_0(n-m)\}}{\{a^{n+4}\}}\right],$$
$$\psi = \frac{-\chi}{\{6a^2(m+n+6)\}}. \quad (7)$$

The parameters χ and ψ can be calculated using (7) with appropriate values of m, n, and b_0 so that the calculated values of elastic constants justify the experimental data.

2.2. Ultrasonic Velocity. The anisotropic behaviour of the material can be understood with the knowledge of ultrasonic

velocity because the velocity is related to the second order elastic constants [17]. On the basis of mode of atomic vibration, there are three types of velocities (longitudinal, quasishear, and shear) in acoustical region [18]. These velocities vary with the direction of propagation of wave from the unique axis of hexagonal-structured crystal [19, 20]. The ultrasonic velocities as a function of angle between direction of propagation and unique axis for hexagonal-structured materials are [21]

$$\begin{aligned} V_L^2 &= \Big\{C_{33}\cos^2\theta + C_{11}\sin^2\theta + C_{44} \\ &\quad + \Big\{\left[C_{11}\sin^2\theta - C_{33}\cos^2\theta + C_{44}\left(\cos^2\theta - \sin^2\theta\right)\right]^2 \\ &\quad + 4\cos^2\theta\sin^2\theta(C_{13}+C_{44})^2\Big\}^{1/2}\Big\}/2\rho, \\ V_{S1}^2 &= \Big\{C_{33}\cos^2\theta + C_{11}\sin^2\theta + C_{44} \\ &\quad - \Big\{\left[C_{11}\sin^2\theta - C_{33}\cos^2\theta + C_{44}\left(\cos^2\theta - \sin^2\theta\right)\right]^2 \\ &\quad + 4\cos^2\theta\sin^2\theta(C_{13}+C_{44})^2\Big\}^{1/2}\Big\}/2\rho \\ V_{S2}^2 &= \frac{\left\{C_{44}\cos^2\theta + C_{66}\sin^2\theta\right\}}{\rho}, \end{aligned} \tag{8}$$

where V_L, V_{S1} and V_{S2} are longitudinal, quasi shear and pure shear wave ultrasonic velocities. Variables ρ and θ represent the density of the material and angle with the unique axis of the crystal, respectively. The Debye temperature (T_D) is an important physical parameter for the characterization of materials, which is well related to the Debye average velocity (V_D):

$$T_D = \frac{\hbar V_D (6\pi^2 n_a)^{1/3}}{k_B}, \tag{9}$$

here

$$V_D = \left\{\frac{1}{3}\left(\frac{1}{V_1^3} + \frac{1}{V_2^3} + \frac{1}{V_3^3}\right)\right\}^{-1/3}, \tag{10}$$

where $\hbar$ is quantum of action and is equal to Planck's constant divided by 2π; k_B is Boltzmann Constant; n_a is atom concentration.

The above formulae have been used for the evaluation of ultrasonic velocity and related parameters for the selected materials.

2.3. Ultrasonic Attenuation and Allied Parameters. The predominant causes for the ultrasonic attenuation in a solid at room temperature are phonon-phonon interaction (Akhieser loss) and thermoelastic relaxation mechanisms. The ultrasonic attenuation coefficient ($\mathcal{A}_{\text{Akh}}$) due to phonon-phonon interaction and thermoelastic relaxation mechanisms is given by the following expression [17, 22]:

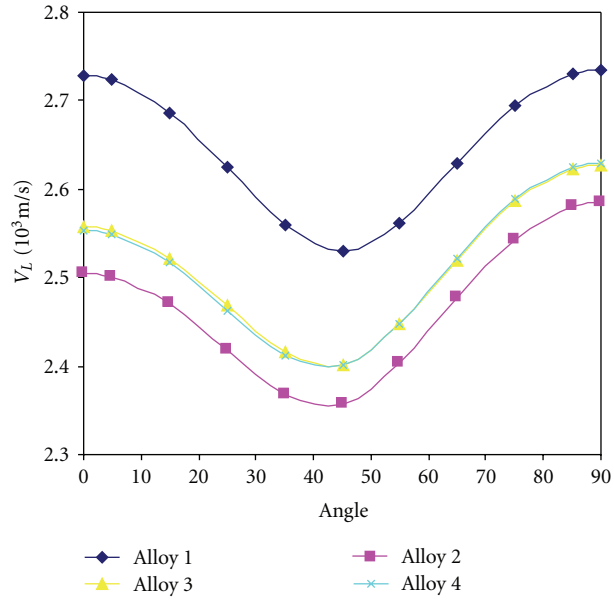

FIGURE 1: V_L versus angle with unique axis of crystal.

$$\left(\frac{\mathcal{A}}{f^2}\right)_{\text{Akh}} = \frac{4\pi^2\left(3E_0\left\langle\left(\gamma_i^j\right)^2\right\rangle - \left\langle\gamma_i^j\right\rangle^2 C_V T\right)\tau}{2\rho V^3}, \tag{11}$$

$$\left(\frac{\mathcal{A}}{f_2}\right)_{\text{Th}} = \frac{4\pi^2\left\langle\gamma_i^j\right\rangle^2 kT}{2\rho V_L^5}, \tag{12}$$

where, f: frequency of the ultrasonic wave; V: ultrasonic velocity for longitudinal and shear wave; V_L: longitudinal ultrasonic velocity; E_0: thermal energy density; γ_i^j : Grüneisen number (i, j are the mode and direction of propagation).

The Grüneisen number for hexagonal-structured crystal along $\langle 001\rangle$ orientation or $\theta = 0^\circ$ is direct consequence of second- and third-order elastic constants. $D = 3(3E_0\langle\gamma_i^j\rangle^2 - \langle\gamma_i^j\rangle^2 C_V T)/E_0$ is known as acoustic coupling constant, which is the measure of acoustic energy converted to thermal energy. When the ultrasonic wave propagates through crystalline material, the equilibrium of phonon distribution is disturbed. The time for reestablishment of equilibrium of the thermal phonon distribution is called thermal relaxation time (τ) and is given by following expression:

$$\tau = \tau_S = \frac{\tau_L}{2} = \frac{3k}{C_V V_D^2}. \tag{13}$$

Here τ_L and τ_S are the thermal relaxation time for longitudinal and shear wave. k and C_V are the thermal conductivity and specific heat per unit volume of the material, respectively.

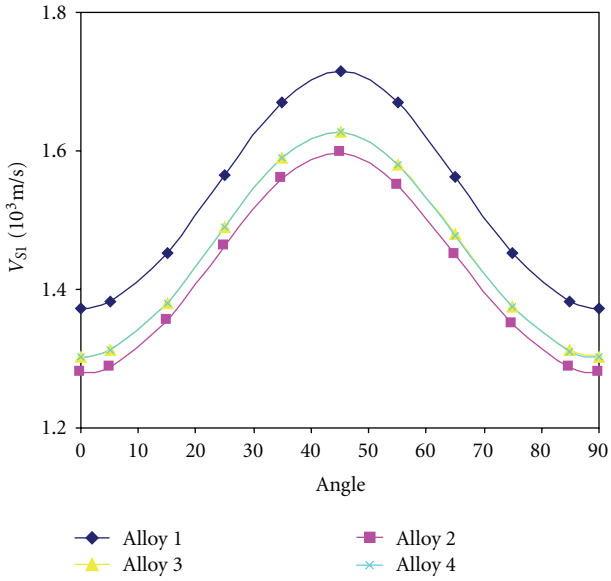

FIGURE 2: V_{S1} versus angle with unique axis of crystal.

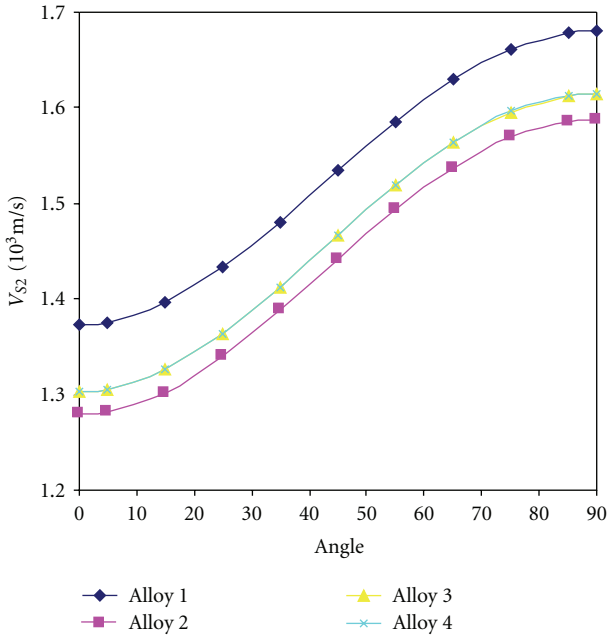

FIGURE 3: V_{S2} versus angle with unique axis of crystal.

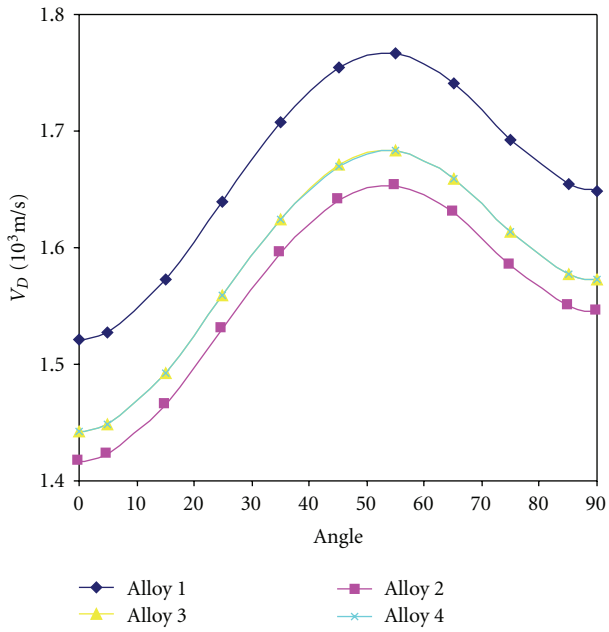

FIGURE 4: V_D versus angle with unique axis of crystal.

3. Results and Discussion

3.1. Higher-Order Elastic Constants. The unit cell parameters "a" (basal plane parameter) and "p" (axial ratio) for $Zr_{100-X}Sn_X$ alloys are 3.17 Å, 3.23 Å, 3.21 Å, 3.21 Å, and 1.622, 1.599, 1.603, 1.600, respectively, [23]. The values of m and n for chosen materials are 6 and 7. The value of b_0 is 1.79×10^{-64} erg cm^7 for all alloys. The SOEC and TOEC have been calculated for these alloys using (4) and are presented in Table 1.

Published theoretical/experimental data on the elastic constants for the chosen alloys are not available for comparison. Comparison for the present values to theoretical/experimental studies of pure metals, as shown in Table 1, demonstrates that results obtained from the present investigation are higher than those of the pure metals as reported by other investigators [24, 25]. The obtained values of the SOEC and TOEC are of the same order as previous experimental and theoretical studies of other metallic alloys and metals [19, 21, 26–28]. Therefore, it is concluded that the theoretical approach to evaluate the SOEC and TOEC is valid for the chosen alloys. The bulk modulus (B) for these alloys can be calculated with the formula $B = 2(C_{11} + C_{12} + 2C_{13} + C_{33}/2)/9$. The evaluated B for these alloys is presented in Table 1.

3.2. Ultrasonic Velocity and Allied Parameters. The density (ρ) and thermal conductivity (k) at room temperature have been taken from the literature [23]. The value of C_V and E_0 are evaluated using tables of physical constants and Debye temperature. The quantities ρ, C_V, E_0, k, and calculated acoustic coupling constants (D_L & D_S) are presented in Table 2.

The calculated orientation-dependent ultrasonic wave velocities and Debye average velocities at 300 K are shown in Figures 1, 2, 3 and 4. Figures 1–3 show that the velocities V_L and V_{S1} have minima and maxima, respectively, at 45° with the unique axis of the crystal while V_{S2} increases with the angle from the unique axis. The combined effect of SOEC and density is reason for abnormal behaviour of angle-dependent velocities.

The nature of the angle-dependent velocity curves in the present work is found similar as that for heavy rare earth metals, Laves-phase compounds, and other hexagonal

Table 1: SOEC, TOEC, and Bulk Modulus (B) in the unit of 10^{10} Nm^{-2} of ZrSn alloys at room temperature.

(a)

Alloys	C_{11}	C_{12}	C_{13}	C_{33}	C_{44}	C_{66}	B
1	22.416	5.505	4.712	22.312	5.652	8.791	10.775
2	19.116	4.694	3.904	17.962	4.683	7.500	9.003
3	20.215	4.964	4.147	19.162	4.974	7.928	9.551
4	20.424	5.015	4.176	19.240	5.009	8.009	9.628
Zr [24]	14.10	6.76	6.43	16.69	2.58	3.68	
Sn [25]	7.01	3.81			3.68		

(b)

Alloys	C_{111}	C_{112}	C_{113}	C_{123}	C_{133}	C_{344}	C_{144}	C_{155}	C_{222}	C_{333}
1	−365.54	−57.96	−12.09	−15.36	−75.37	−70.66	−17.90	−11.93	−289.23	−278.90
2	−311.73	−49.42	−10.01	−12.73	−60.67	−56.88	−14.83	−9.88	−246.65	−218.15
3	−329.65	−52.26	−10.64	−13.52	−64.72	−60.68	−15.75	−10.50	−260.83	−233.73
4	−333.06	−52.81	−10.71	−13.61	−64.99	−60.92	−15.86	−10.57	−263.52	−233.95

Table 2: Density (ρ: in 10^3 kg m^{-3}), specific heat per unit volume (C_V: in 10^6 Jm^{-3}K^{-1}), thermal energy density (E_0: in 10^8 Jm^{-3}), thermal conductivity (k: in Wm^{-1}K^{-1}), and acoustic coupling constant (D_L, D_S) of ZrSn alloys.

Alloys	ρ	C_V	E_0	k	D_L	D_S
1	29.97	7.33	15.12	5.47	57.36	1.11
2	28.61	7.05	14.92	5.08	56.41	1.19
3	29.28	7.14	15.04	4.56	56.30	1.16
4	29.53	7.15	15.06	4.21	56.37	1.18

wurtzite structured materials (GaN, AlN, InN) [13, 17, 19, 21, 22, 28]. Thus, the computed velocities for these alloys are justified.

Debye average velocities (V_D) of these alloys are increasing with the angle and have maxima at 55° at 300 K (Figure 4). Since V_D is calculated using V_L, V_{S1}, and V_{S2} [13, 22]; therefore, the angle variation of V_D is influenced by the constituent ultrasonic velocities. The maximum V_D at 55° is due to a significant increase in longitudinal and pure shear (V_{S2}) wave velocities and a decrease in quasishear (V_{S1}) wave velocity. Thus, it can be concluded that when a sound wave travels at 55° with the unique axis of these alloys then the average sound wave velocity is maximum.

Thus, the present average sound velocity directly correlates with the Debye temperature, specific heat, and thermal energy density of theses materials.

The calculated thermal relaxation time is visualised in Figure 5. The angle-dependent thermal relaxation time curves follow the reciprocal nature of V_D as $\tau \propto 3\,\mathrm{K}/C_V V_D^2$. This implies that τ for these are mainly affected by the thermal conductivity. The τ for hexagonal-structured materials is the order of picoseconds [19]. Hence, the calculated τ justifies the hcp structure of chosen alloys at room temperature. The minimum τ for wave propagation along $\theta = 55°$ implies that the reestablishment time for the equilibrium distribution of thermal phonons will be minimum for propagation of wave along this direction. The value of thermal conductivity of alloy: 3 is greater than alloy: 4. So, in Figures 1–4, the ultrasonic velocities of alloy 3 and alloy 4 seem quasi-identical, but in Figure 5, their relaxation times differ.

Table 3: Ultrasonic attenuation coefficient (in 10^{-17} Nps^{2}m^{-1}) of ZrSn alloys.

Alloys	1	2	3	4
$(\mathcal{A}/f^2)_{\mathrm{Th}}$	0.115	0.510	0.404	0.373
$(\mathcal{A}/f^2)_L$	362.491	529.937	417.917	385.668
$(\mathcal{A}/f^2)s$	27.497	42.024	32.513	30.404
$(\mathcal{A}/f^2)_{\mathrm{Total}}$	390.103	572.471	450.834	416.445

3.3. Ultrasonic Attenuation. In the evaluation of ultrasonic attenuation, it is supposed that wave is propagating along the unique axis (⟨001⟩ direction) of these alloys. The attenuation coefficient over frequency square $(\mathcal{A}/f^2)_{\mathrm{Akh}}$ for longitudinal $(\mathcal{A}/f^2)_L$ and shear wave $(\mathcal{A}/f^2)_S$ are calculated using (11) under the condition $\omega\tau \ll 1$ at room temperature. The thermoelastic loss over frequency square $(\mathcal{A}/f^2)_{\mathrm{th}}$ is calculated with (12). The values of $(\mathcal{A}/f^2)_L$, $(A/f^2)_S$, $(\mathcal{A}/f^2)_{\mathrm{th}}$, and total attenuation $(\mathcal{A}/f^2)_{\mathrm{Total}}$, are presented in Table 3.

Table 3 indicates that the thermoelastic loss is very small in comparison to Akhieser loss, and ultrasonic attenuation for longitudinal wave $(\mathcal{A}/f^2)_L$ is greater than that of shear wave $(\mathcal{A}/f^2)_S$. This reveals that ultrasonic attenuation due to phonon-phonon interaction along longitudinal wave is governing factor for total attenuation ($(\mathcal{A}/f^2)_{\mathrm{Total}} = (\mathcal{A}/f^2)_{\mathrm{Th}} + (\mathcal{A}/f^2)_L + (\mathcal{A}/f^2)_S$). The total attenuation is

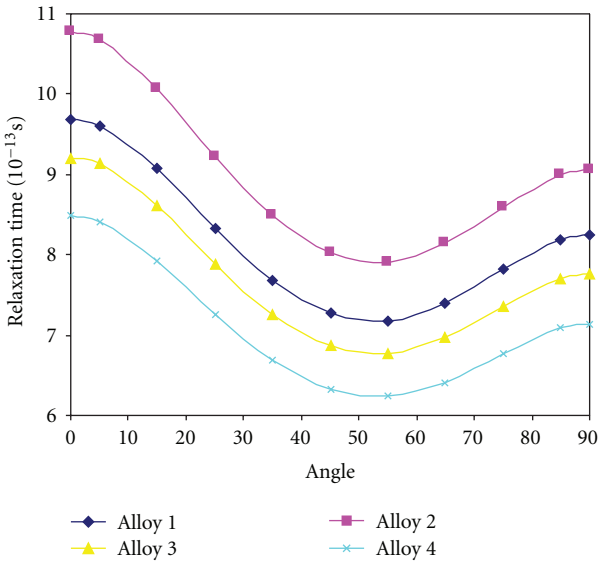

FIGURE 5: Relaxation time versus angle with unique axis of crystal.

mainly affected by thermal energy density and thermal conductivity. Thus, it may predict that at 300 K the alloy 1 behaves as its purest form and is more ductile as evinced by minimum attenuation while alloy 2 is least ductile. Therefore impurity will be least in the alloy 1 at room temperature.

Since $\mathcal{A} \propto V^{-3}$ and velocity is the largest for alloy 1 among alloy 2; thus, the attenuation $\mathcal{A}$ should be smallest and material should be most ductile. The minimum ultrasonic attenuation for alloy 1 justifies its quite stable hcp structure state. The total attenuation of these alloys are much larger than third-group nitrides (AlN: $4.441 \times 10^{-17}\,\mathrm{Nps^2m^{-1}}$, GaN: $14.930 \times 10^{-17}\,\mathrm{Nps^2m^{-1}}$, and InN: $20.539 \times 10^{-17}\,\mathrm{Nps^2m^{-1}}$) due to their large thermal conductivity and acoustic coupling constants [19, 29]. This implies that the interaction between acoustical phonon and quanta of lattice vibration for these alloys is large in comparison to third-group nitrides.

4. Conclusions

Based on the above discussion it is worthwhile to state the following:

(i) The present method to evaluate second- and third-order elastic constants involving many body interaction potential for hexagonal wurtzite crystal structured materials (alloys) is correct.

(ii) All elastic constants and density are mainly the affecting factor for anomalous behaviour of ultrasonic velocity in these alloys.

(iii) When a sound wave travels at 55° with the unique axis of these crystals, then the average sound wave velocity is maximum. Since the Debye average velocity is calculated using the constituent velocities V_L, V_{S1}, and V_{S2}, hence, a good resemblance in V_D implies that our calculated velocities are correct.

(iv) The ⟨001⟩ direction is the direction of symmetry for these alloys as they have the same quasishear and pure shear wave velocities.

(v) The order of thermal relaxation time for these alloys is found in picoseconds, which justifies their hcp structure at 300 K. The reestablishment time for the equilibrium distribution of thermal phonons will be minimum for the wave propagation along $\theta = 55°$ due to being the smallest value of τ along this direction.

(vi) The acoustic coupling constant of these alloys for longitudinal wave are found five times larger than third-group nitrides. Hence, the conversion of acoustic energy into thermal energy will be large for these alloys. This shows general suitability of chosen alloys.

(vii) The ultrasonic attenuation due to phonon-phonon interaction mechanism is predominant over total attenuation as a governing factor of thermal conductivity.

(viii) $Zr_{82}Sn_{18}$ alloy is more suitable for industrial and other uses, as it has the highest elastic constants as well as wave velocity in comparison to other chosen alloys.

(ix) The mechanical and ultrasonic properties of these alloys will be better than pure Zr and Sn due to their high SOEC and ultrasonic velocity and low ultrasonic attenuation.

Thus, obtained results in the present work can be used for further investigations, general and industrial applications. Our theoretical approach is valid for ultrasonic characterization of these materials at room temperature. The ultrasonic behavior in these alloys as discussed above shows important microstructural characteristic feature, which is well connected to thermoelectric properties of the materials. These results, together with other well-known physical properties, may expand future prospects for the application and study of these materials.

Acknowledgments

The author wishes to express sincere thanks to Dr. Ashok K. Chauhan, President, AMITY School of Engineering and Technology (ASET), New Delhi, Prof. B. P. Singh, Senior Director, ASET New Delhi, and Prof. S. K. Kor and Prof. Raja Ram Yadav, Department of Physics, Allahabad University, for encouraging and providing necessary facilities in carrying out the work.

References

[1] J. S. Gyanchandani, S. C. Gupta, S. K. Sikka, and R. Chidambaram, "Structural stability of hafnium under pressure," *Journal of Physics*, vol. 2, no. 30, Article ID 011, pp. 6457–6459, 1990.

[2] J. S. Gyanchandani, S. C. Gupta, S. K. Sikka, and R. Chidambaram, "The equation of state and structural stability of

titanium obtained using the linear muffin-tin orbital band-structure method," *Journal of Physics*, vol. 2, no. 2, pp. 301–305, 1990.

[3] A. L. Kutepov and S. G. Kutepova, "Crystal structures of Ti under high pressure: theory," *Physical Review B*, vol. 67, no. 13, article 132102, 2003.

[4] R. Ahuja, L. Dubrovinsky, N. Dubrovinskaia et al., "Titanium metal at high pressure: synchrotron experiments and ab initio calculations," *Physical Review B*, vol. 69, no. 18, article 184102, 2004.

[5] D. Young, *Phase Diagrams of the Elements*, University of California Press, Berkeley, Calif, USA, 1991.

[6] P. Villars and L. D. Calvert, Eds., *Pearson's Handbook of Crystallographic Data for Intermetallic Phases*, American Society for Metals, Materials Park, Ohio, USA, 2nd edition, 1991.

[7] G. Simmons and H. Wang, *Single Crystal Elastic Constants and Calculated Aggregate Properties: A Handbook*, MIT Press, Cambridge, Mass, USA, 2nd edition, 1971.

[8] E. Clouet, J. M. Sanchez, and C. Sigli, "First-principles study of the solubility of Zr in Al," *Physical Review B*, vol. 65, no. 9, article 094105, 2002.

[9] I. Schnell, M. D. Jones, S. P. Rudin, and R. C. Albers, "Tight-binding calculations of the elastic constants and phonons of hcp Zr: complications due to anisotropic stress and long-range forces," *Physical Review B*, vol. 74, no. 5, article 054104, 2006.

[10] D. J. Oh and R. A. Johnson, "Relationship between c/a ratio and point defect properties in HCP metals," *Journal of Nuclear Materials*, vol. 169, pp. 5–8, 1989.

[11] Y. M. Kim, B. J. Lee, and M. I. Baskes, "Modified embedded-atom method interatomic potentials for Ti and Zr," *Physical Review B*, vol. 74, no. 1, article 014101, 2006.

[12] M. I. Baskes and R. A. Johnson, "Modified embedded atom potentials for HCP metals," *Modelling and Simulation in Materials Science and Engineering*, vol. 2, no. 1, pp. 147–163, 1994.

[13] P. K. Yadawa, D. Singh, D. K. Pandey, and R. R. Yadav, "Elastic and acoustic properties of heavy rare-earth metals," *The Open Acoustics Journal*, vol. 2, no. 1, pp. 61–67, 2009.

[14] D. Singh and P. K. Yadawa, "Effect of platinum addition to coinage metals on their ultrasonic properties," *Platinum Metals Review*, vol. 54, no. 3, pp. 172–179, 2010.

[15] P. Ravindran, L. Fast, P. A. Korzhavyi, B. Johansson, J. Wills, and O. Eriksson, "Density functional theory for calculation of elastic properties of orthorhombic crystals: application to $TiSi_2$," *Journal of Applied Physics*, vol. 84, no. 9, pp. 4891–4904, 1998.

[16] L. Louail, D. Maouche, A. Roumili, and F. A. Sahraoui, "Calculation of elastic constants of 4d transition metals," *Materials Letters*, vol. 58, no. 24, pp. 2975–2978, 2004.

[17] A. K. Yadav, R. R. Yadav, D. K. Pandey, and D. Singh, "Ultrasonic study of fission products precipitated in the nuclear fuel," *Materials Letters*, vol. 62, no. 17-18, pp. 3258–3261, 2008.

[18] C. Oligschleger, R. O. Jones, S. M. Reimann, and H. R. Schober, "Model interatomic potential for simulations in selenium," *Physical Review B*, vol. 53, no. 10, pp. 6165–6173, 1996.

[19] D. K. Pandey, D. Singh, and R. R. Yadav, "Ultrasonic wave propagation in IIIrd group nitrides," *Applied Acoustics*, vol. 68, no. 7, pp. 766–777, 2007.

[20] S. K. Verma, R. R. Yadav, A. K. Yadav, and B. Joshi, "Non-destructive evaluations of gallium nitride nanowires," *Materials Letters*, vol. 64, no. 15, article 11226, 2010.

[21] D. K. Pandey, P. K. Yadawa, and R. R. Yadav, "Acoustic wave propagation in Laves-phase compounds," *Materials Letters*, vol. 61, no. 25, pp. 4747–4751, 2007.

[22] D. K. Pandey, P. K. Yadawa, and R. R. Yadav, "Ultrasonic properties of hexagonal ZnS at nanoscale," *Materials Letters*, vol. 61, no. 30, pp. 5194–5198, 2007.

[23] D. Biswas, A. K. Meikap, S. K. Chattopadhyay, and S. K. Chatterjee, "Low-temperature electrical transport properties of disordered $Zr_{100-x}Sn_x$ alloys," *Physica B*, vol. 382, no. 1-2, pp. 51–57, 2006.

[24] Y.-J. Hao, L. Zhang, X.-R. Chen, Y.-H. Li, and H.-L. He, "Phase transition and elastic constants of zirconium from first-principles calculations," *Journal of Physics*, vol. 20, no. 23, article 235230, 2008.

[25] A. Berroukche, B. Soudini, and K. Amara, "Molecular dynamics simulation study of structural, elastic and thermodynamic properties of tin below 286K," *International Journal of Nanoelectronics and Materials*, vol. 1, no. 1, pp. 41–51, 2008.

[26] B. Magyari-Kope, L. Vitos, and G. Grimvall, "Perturbative quantum-state estimation anomalous behaviour of lattice parameters and elastic constants in hcp Ag-Zn alloys," *Physical Review B*, vol. 77, article 052102, 2004.

[27] Y. Matsuo, "Elastic behavior and phase stability in the H.C.P. ε-phase of Ag-Zn alloy," *Journal of the Physical Society of Japan*, vol. 53, no. 4, pp. 1360–1365, 1984.

[28] D. K. Pandey, D. Singh, and P. K. Yadawa, "Ultrasonic study of osmium and ruthenium," *Platinum Metals Review*, vol. 53, no. 2, pp. 91–97, 2009.

[29] H. Landolt and R. Bornstein, *Landolt-Bornstein: Numerical Data and Function Relationship in Science and Technology. Group III*, vol. 11, Springer, Berlin, Germany, 1979.